

# Xnlbd: A NEW PYTHON PACKAGE FOR THE ANALYSIS OF NON-LINEAR BEAM DYNAMICS PHENOMENA\*

D. E. Veres<sup>1†</sup>, F. Capoani, M. Giovannozzi, C. E. Montanari<sup>2</sup>, CERN, Geneva, Switzerland  
 G. Franchetti<sup>1</sup>, GSI Helmholtzzentrum für Schwerionenforschung, Darmstadt, Germany  
 A. Bazzani, Dipartimento di Fisica e Astronomia, Università di Bologna, and INFN, Bologna, Italy  
 M. N. Vrahatis, Department of Mathematics, University of Patras, Patras, Greece  
<sup>1</sup>also at Goethe University, Frankfurt am Main, Germany  
<sup>2</sup>also at University of Manchester, Manchester, United Kingdom

## Abstract

Non-linear effects in particle accelerators have historically been treated as harmful influences that necessitate various mitigation schemes. Therefore, the simulation tools available are largely focused on identifying and correcting resonances. However, recent advances proved that non-linear beam dynamics enables new techniques for manipulating particle beams and can characterise diffusion and chaos in particle accelerators. The simulation tools currently available for these purposes are difficult to integrate across different frameworks. This paper presents Xnlbd, a new Python package extending the Xsuite simulation framework, which aims to provide a unified set of tools for analysing non-linear beam dynamics phenomena. It allows the visualisation of highly non-linear phase spaces, the efficient finding of both stable and unstable fixed points and separatrices, the calculation of resonance driving terms and normal forms, and the computation of dynamic indicators for the detection of chaotic motion.

## INTRODUCTION

In recent times, the study of non-linear beam dynamics has unveiled the potential associated with the intricate phase-space structures resulting from non-linear phenomena. These structures encompass both stable and unstable fixed points created by non-linear resonances, as well as separatrices that link these unstable fixed points. The separatrices form phase-space regions where processes such as adiabatic trapping and transport occur through slow variation of accelerator parameters. These principles are fundamental to the CERN PS Multi-Turn Extraction (MTE) [1–3] and various proposed non-linear beam manipulations [4–7]. The determination of the regular or chaotic character of an orbit is yet another important indicator of beam dynamics.

Implementing these concepts requires the use of modern computational tools. CERN has embarked on significant efforts to develop Xsuite, a new Python-based simulation framework tailored for accelerator physics [8]. This initiative now includes the creation of a specialised package, called Xnlbd, to further support applications in non-linear beam dynamics.

## COMPUTATION OF FIXED POINTS AND SEPARATRICES

The computation of fixed points of non-linear mappings is a condition *sine qua non* for analysing and studying non-linear beam dynamics. It is worth mentioning that in 1883 and 1884 Poincaré, in his work on the three-body problem, proposed without proof an important theorem for the existence of fixed points of continuous mappings from an  $N$  dimensional cube (parallelootope) into  $\mathbb{R}^N$ . Poincaré's theorem was proved by Miranda in 1940 [9], and is called the Bolzano-Poincaré-Miranda theorem or Poincaré-Miranda theorem. In 1989, a short proof and a generalisation of this theorem was given by invoking the principle of homotopic invariance of topological degree [10]. In 2020, in the context of the existence of unstable periodic solutions of dynamical systems, the theorem was named the Miranda-Vrahatis theorem [11].

A point  $x$  is a fixed point of order  $q$  if the vector function  $f(x) = M^q(x) - x$  vanishes, where  $M^q(x)$  is the one-turn map applied  $q$  times to  $x$ .  $M(x)$  is obtained by numerical tracking. Fixed points are classified as elliptic (stable), hyperbolic (unstable), or parabolic according to the eigenvalues of the Jacobian matrix. Applying traditional iterative root-finding algorithms (e.g. Newton's method) can work for stable fixed points. However, they generically fail for unstable fixed points. The algorithm in Xnlbd adopted the approach of [12], described in detail in [13, 14].

The core idea is to apply bisection to refine an initial guess of the fixed-point position using topological degree theory. This approach relies only on the sign of the components of  $f(x)$ , and is thus unaffected by the growing function values in the vicinity of unstable fixed points. In the 1D case, given two initial guesses  $x_1$  and  $x_2$ , a fixed point  $x_{fp} \in (x_1, x_2)$  exist if  $\text{sgn}(f(x_1)) \text{sgn}(f(x_2)) < 0$ , where  $\text{sgn}$  is the signum function. If fulfilled, one can apply bisection to converge to the fixed point.

Extension to higher dimensions is straightforward, e.g. in 2D,  $f(x)$  has two components, leading to four possible overall sign configurations,  $(++)$ ,  $(+-)$ ,  $(-+)$ ,  $(--)$ , while in  $N$  dimensions we have  $2^N$  possible sign configurations. An  $N$ -polyhedron with  $2^N$  vertices, each with a different sign configuration such that along each edge only one component of  $f(x)$  changes sign is a characteristic  $N$ -polyhedron. Starting from a characteristic  $N$ -polyhedron, bisection along

\* Work supported by the Wolfgang Gentner Programme of the German Federal Ministry of Education and Research (grant no. 13E18CHA).

† dora.erzsebet.veres@cern.ch

all edges can be performed, leaving the resulting reduced  $N$ -polyhedron characteristic. This characteristic bisection can then be repeated until the fixed point, estimated as the midpoint of the longest diagonal of the characteristic  $N$ -polyhedron, reaches the desired accuracy. The concepts of a characteristic  $N$ -polyhedron and characteristic bisection have been introduced in [15] and have been effectively applied in a wide range of problems including non-linear dynamics.

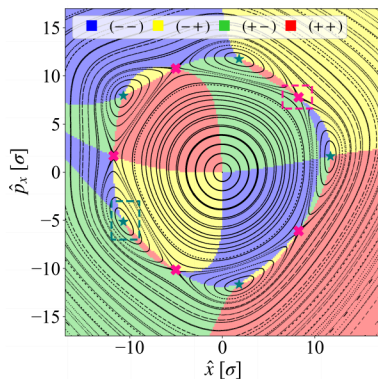


Figure 1: Horizontal phase space of the Hénon map close to a fifth-order resonance coloured according to the sign of  $f(x)$ . The map's orbits are also overlaid. Stable and unstable fixed points are shown in teal and pink, respectively, along with the dashed rectangles used as initial polygons for the fixed-point search.

To illustrate the `Xn1bd` implementation, it is useful to assign colours to the possible sign configurations and colour the phase space accordingly, as illustrated in Fig. 1, for a 2D example using the Hénon map close to a fifth-order resonance. Obviously, the fixed points are located at the intersections of all colours. The algorithm in `Xn1bd` takes the following steps to construct the characteristic  $N$ -polyhedron:

1. A rough estimate of the fixed point is found in the user-provided  $N$ -polyhedron by searching for the intersection of all  $2^N$  colours on a user-defined grid. If multiple intersections are present, only one is selected at random.
2.  $10^N$  points are randomly uniformly sampled on the surface of an  $N$ -dimensional hypersphere centred around the rough fixed point estimate. The radius is chosen to be of the same order of magnitude as the grid step to ensure a single intersection in the hypersphere.
3. The colour of each of these  $10^N$  points is evaluated, and  $2^N$  points of distinct colour are selected as vertices of the characteristic  $N$ -polyhedron in the proper order.

Note that the sequence of appearance of the colours determines the stability of a fixed point, which can be used for the localisation and computation of fixed points of a specific stability type. Figure 1 shows an example of the described algorithm. `Xn1bd` can compute fixed points in 2, 4, or 6 dimensions of any line object constructed by `Xsuite`.

To design beam manipulations based on non-linear beam dynamics, it is often necessary to find the separatrix delimiting regions of phase space. In `Xn1bd` an approximation of

the separatrix is obtained by tracking initial conditions close to an unstable fixed point. `Xn1bd` returns the approximate separatrix of each identified region of the phase space, as well as their area  $A$ . The separatrix can be obtained for arbitrary resonance order and even for islands generated by a time-dependent exciter, as illustrated in Fig. 2.

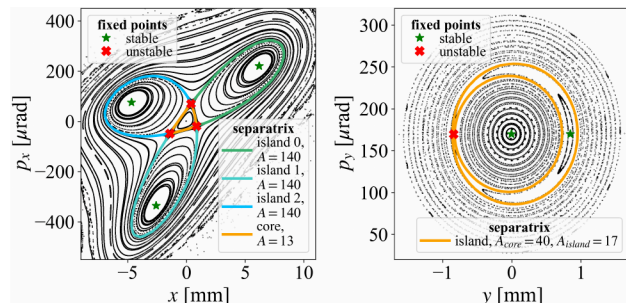


Figure 2: Fixed points and approximate separatrices in horizontal phase space obtained with `Xn1bd` at the SPS betatron collimator for non-zero momentum offset close to the third-order resonance (left), and at LHC IP1 in the presence of a vertical AC dipole (right).

## BIRKHOFF NORMAL FORMS

For the computation of the Birkhoff normal form, the 4D one-turn map of the lattice is first computed. `Xn1bd` contains polynomial-form implementations of the beam elements most frequently used in `Xsuite` (work to implement the remaining elements is ongoing), as well as a Hénon map element unique to `Xn1bd`. The one-turn map of the desired polynomial order is evaluated by efficiently computing the composition of the maps of the ring lattice.

The normal form calculation is performed via a Python implementation of ARES [16], which solves the equation

$$\Phi \circ U = F \circ \Phi, \quad (1)$$

where  $U$  is the normal form,  $\Phi$  is the conjugating function (tangent to the identity), and  $F$  is the one-turn map, which is assumed to have an elliptic fixed point at the origin. Using complex normalised Courant-Snyder coordinates  $z$ , the linear part can be diagonalised and the map reads

$$F(z) = \mathbf{A}_\omega z + \sum_{n \geq 2} [F(z)]_n. \quad (2)$$

Here,  $\mathbf{A}_\omega = (e^{i\omega_1}, e^{-i\omega_1}, e^{i\omega_2}, e^{-i\omega_2})$  is the diagonal matrix of eigenvalues and  $[\cdot]_n$  represents the  $n$ th-order homogenous polynomial component of  $F$ . Eq. (1) can be solved using an order-by-order approach, truncating at a chosen order.  $U$  and  $\Phi$  are represented as Lie transformations  $U(\zeta) = \mathbf{A}_\omega e^{D_A} \zeta$  and  $\Phi(\zeta) = e^{D_G} \zeta$ , where  $\zeta$  is the vector in the normal-form coordinates and the action of the operator  $D_X$  is defined by Poisson bracket, i.e.  $D_X Y(\zeta) = \{Y, X\}$ . The Lie transformation  $e^{D_X} Y$  is obtained by a recursive algorithm. This representation allows calculating the compositions in Eq. (1) as  $F(\Phi(\zeta)) = e^{D_G} F(\zeta)$

and  $\Phi(U(\zeta)) = e^{D_A} \Phi(\Lambda_\omega \zeta)$ . The mathematical details for determining the solution of Eq. (1) can be found in [17]

To extract important information about particle dynamics, the interpolating Hamiltonian is also computed [17]. Its flow interpolates the orbits of  $U$  at integer times. The amplitude-detuning terms and resonance-driving terms can then be extracted from the interpolating Hamiltonian.

The algorithm allows computing the normal forms in non-resonant, exactly resonant, and quasi-resonant cases, for single and double resonances. Figure 3 shows examples of orbits of the quasi-resonant (top) and non-resonant (bottom) Hénon map in physical (left), transformed into normalised Courant-Snyder (centre) and normal-form (right) coordinates. The Hamiltonian contours in normal-form coordinates are also overlaid with coloured, dashed lines.

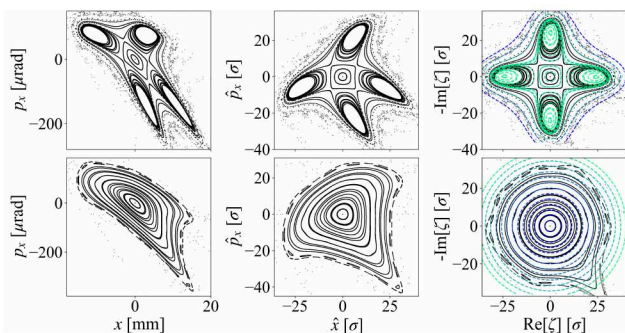


Figure 3: Hénon map orbits in physical space, Courant-Snyder normalised coordinates and normal-form coordinates (left to right). Quasi-resonant (top) and non-resonant (bottom) cases are shown. The contours of the interpolating Hamiltonian returned by Xn1bd are also plotted on the right-most panels with coloured, dashed lines.

## CHAOS INDICATORS

Chaos indicators are widely studied in various fields of science including non-linear dynamics [18–23]. In accelerator physics, Frequency Map Analysis (FMA) [24, 25] has gained traction in this domain (see, e.g. [26–28]), while Fast Lyapunov Indicators (FLI) [20] and their improved versions, such as the Birkhoff-weighted FLI (FLI<sup>WB</sup>) [29], remain underused in accelerator lattice optimisation studies.

The Xn1bd package includes a suite of chaos indicators: FLI with and without Birkhoff weights, Reverse Error Method (REM) [19], FMA, and the Generalized Alignment Index (GALI) [30]. FMA is evaluated using the average phase advance method with Birkhoff weights [29, 31], offering a memory-efficient alternative to FFT-based methods and allowing real-time computations without excessive data storage on GPU devices. Unlike previous studies that focus on theoretical comparisons of indicators [22] (applied to the Hénon map) or the application to a realistic accelerator lattice [23], this study aims at their efficient implementation and integration in Python-based, GPU-accelerated workflows of the Xsuite framework. A key component is the GPU-based shadow-particle method, built directly on top

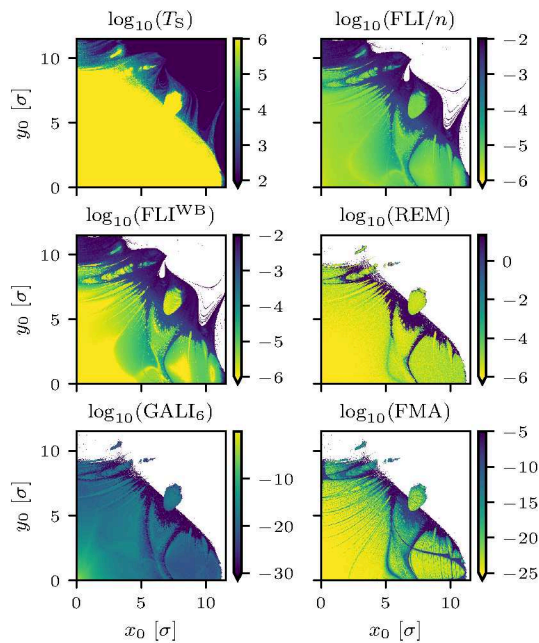


Figure 4: Example of a stability plot (top-left,  $T_s$  being the stability time of an initial condition) together with the chaos indicators evaluated at  $10^6$  turns on an HL-LHC lattice.

of Xobjects [32], which efficiently computes FLI, FLI<sup>WB</sup>, and GALI by tracking and renormalising the separation between nearby trajectories across phase space. By seamlessly integrating with the actively evolving Xsuite framework, which increasingly incorporates features from established tools such as MAD-X, Xn1bd enables the practical use of chaos indicators in modern accelerator optimisation workflows. An example application to a High Luminosity LHC lattice is shown in Fig. 4, illustrating how Xn1bd enables chaos diagnostics for accelerator design studies.

## CONCLUSIONS AND OUTLOOK

The package Xn1bd (<https://github.com/xsuite/xn1bd/>) incorporates a variety of advanced techniques from dynamical system theory. These functionalities are expected to be crucial in advancing the non-linear beam manipulations currently under investigation at CERN.

## ACKNOWLEDGEMENTS

The authors thank J. Dilly and P. Majoros for their advice.

## REFERENCES

- [1] R. Cappi and M. Giovannozzi, “Novel Method for Multiturn Extraction: Trapping Charged Particles in Islands of Phase Space”, *Phys. Rev. Lett.*, vol. 88, no. 10, p. 104801, 2002. doi:10.1103/PhysRevLett.88.104801
- [2] J. Borburgh *et al.*, “First implementation of transversely split proton beams in the CERN Proton Synchrotron for the fixed-target physics programme”, *EPL*, vol. 113, no. 3, 34001. 6 p, 2016. doi:10.1209/0295-5075/113/34001

- [3] A. Huschauer *et al.*, “Transverse beam splitting made operational: Key features of the multiturn extraction at the CERN Proton Synchrotron”, *Phys. Rev. Accel. Beams*, vol. 20, no. 6, p. 061001, 2017.  
doi:10.1103/PhysRevAccelBeams.20.061001
- [4] A. Bazzani, F. Capoani, and M. Giovannozzi, “Analysis of adiabatic trapping phenomena for quasi-integrable area-preserving maps in the presence of time-dependent excitors”, *Phys. Rev. E*, vol. 106, no. 3, p. 034204, Sep. 2022.  
doi:10.1103/PhysRevE.106.034204
- [5] A. Bazzani *et al.*, “Manipulation of transverse emittances in circular accelerators by crossing nonlinear 2D resonances”, *Eur. Phys. J. Plus*, vol. 137, no. 5, p. 594, 2022.  
doi:10.1140/epjp/s13360-022-02797-2
- [6] M. Giovannozzi *et al.*, “A novel non-adiabatic approach to transition crossing in a circular hadron accelerator”, *Eur. Phys. J. Plus*, vol. 136, no. 11, p. 1189, 2021.  
doi:10.1140/epjp/s13360-021-02181-6
- [7] A. Bazzani, F. Capoani, M. Giovannozzi, and R. Tomás, “Non-linear cooling of an annular beam distribution”, *Phys. Rev. Accel. Beams*, vol. 26, no. 2, p. 024001, Feb. 2023.  
doi:10.1103/PhysRevAccelBeams.26.024001
- [8] G. Iadarola *et al.*, “Xsuite: an integrated beam physics simulation framework”, *arXiv*, 2023.  
doi:10.48550/arXiv.2310.00317
- [9] C. Miranda, “Un’osservazione su un teorema di Brouwer, (in italian)”, *Boll. Un. Mat. Ital. II*, vol. 3, pp. 5–7, 1940.
- [10] M. N. Vrahatis, “A short proof and a generalization of Miranda’s existence theorem”, *Proc. Amer. Math. Soc.*, vol. 107, no. 3, pp. 701–703, 1989. doi:10.2307/2048168
- [11] B. Bánhelyi, T. Csendes, and L. Hatvani, “On the existence and stabilization of an upper unstable limit cycle of the damped forced pendulum”, *J. Comput. Appl. Math.*, vol. 371, pp. 112702, 9, 2020. doi:10.1016/j.cam.2019.112702
- [12] M. N. Vrahatis, “CHABIS: a mathematical software package for locating and evaluating roots of systems of nonlinear equations”, *ACM Trans. Math. Softw.*, vol. 14, no. 4, pp. 330–336, 1988. doi:10.1145/50063.51906
- [13] M. N. Vrahatis, “Solving systems of nonlinear equations using the nonzero value of the topological degree”, *ACM Trans. Math. Softw.*, vol. 14, no. 4, pp. 312–329, 1988.  
doi:10.1145/50063.214384
- [14] M. N. Vrahatis, “An efficient method for locating and computing periodic orbits of nonlinear mappings”, *J. Comput. Phys.*, vol. 119, no. 1, pp. 105–119, 1995.  
doi:10.1006/jcph.1995.1119
- [15] M. N. Vrahatis, “The topological degree and the generalized method of bisection for solving systems of nonlinear equations, (in greek)”, Ph.D. thesis, Department of Mathematics, University of Patras, Patras, Greece, 1982.
- [16] A. Bazzani, M. Giovannozzi, and E. Todesco, “A program to compute Birkhoff normal forms of symplectic maps in  $\mathbb{R}^{4n}$ ”, *Comput. Phys. Commun.*, vol. 86, no. 1, pp. 199–207, 1995.  
doi:10.1016/0010-4655(94)00140-W
- [17] A. Bazzani, G. Servizi, E. Todesco, and G. Turchetti, *A normal form approach to the theory of nonlinear betatronic motion*. Geneva: CERN, 1994.  
doi:10.5170/CERN-1994-002
- [18] F. Panichi, L. Ciotti, and G. Turchetti, “Fidelity and reversibility in the restricted three body problem”, *Communications in Nonlinear Science and Numerical Simulation*, vol. 35, pp. 53–68, 2016. doi:10.1016/j.cnsns.2015.10.016
- [19] F. Panichi, K. Goździewski and G. Turchetti, “The reversibility error method (REM): a new, dynamical fast indicator for planetary dynamics”, *MNRAS*, vol. 468, no. 1, pp. 469–491, Jun. 2017. doi:10.1093/mnras/stx374
- [20] M. Guzzo and E. Lega, “Theory and applications of fast Lyapunov indicators to model problems of celestial mechanics”, *Celestial Mech. Dyn. Astron.*, vol. 135, no. 4, p. 37, 2023.  
doi:10.1007/s10569-023-10152-5
- [21] K. Hwang, C. Mitchell, and R. Ryne, “Rapidly converging chaos indicator for studying dynamic aperture in a storage ring with space charge”, *Phys. Rev. Accel. Beams*, vol. 23, no. 8, p. 084601, Aug. 2020.  
doi:10.1103/PhysRevAccelBeams.23.084601
- [22] A. Bazzani, M. Giovannozzi, C. E. Montanari, and G. Turchetti, “Performance analysis of indicators of chaos for nonlinear dynamical systems”, *Phys. Rev. E*, vol. 107, no. 6, p. 064209, Jun. 2023.  
doi:10.1103/PhysRevE.107.064209
- [23] C. E. Montanari *et al.*, “Chaos indicators for non-linear dynamics in circular particle accelerators”, *arXiv*, 2025.  
doi:10.48550/arXiv.2504.12741
- [24] J. Laskar, “Frequency map analysis of an Hamiltonian system”, in *AIP conference proceedings*, pp. 130–159, 1995.  
doi:10.1063/1.48978
- [25] Y. Papaphilippou and J. Laskar, “Frequency map analysis and global dynamics in a galactic potential with two degrees of freedom.”, *Astron. Astrophys.*, vol. 307, pp. 427–449, 1996.  
doi:10.1007/978-94-011-4673-9\_70
- [26] D. Shatilov, E. Levichev, E. Simonov, and M. Zobov, “Application of frequency map analysis to beam-beam effects study in crab waist collision scheme”, *Phys. Rev. ST Accel. Beams*, vol. 14, no. 1, p. 014001, Jan. 2011.  
doi:10.1103/PhysRevSTAB.14.014001
- [27] Y. Papaphilippou, “Detecting chaos in particle accelerators through the frequency map analysis method”, *Chaos*, vol. 24, no. 2, p. 024412, 2014. doi:10.1063/1.4884495
- [28] P. Zisopoulos, Y. Papaphilippou, and J. Laskar, “Refined betatron tune measurements by mixing beam position data”, *Phys. Rev. Accel. Beams*, vol. 22, no. 7, p. 071002, Jul. 2019.  
doi:10.1103/PhysRevAccelBeams.22.071002
- [29] S. Das and J. A. Yorke, “Super convergence of ergodic averages for quasiperiodic orbits”, *Nonlinearity*, vol. 31, no. 2, pp. 491–501, Jan. 2018.  
doi:10.1088/1361-6544/aa99a0
- [30] Ch. Skokos and T. Manos, *The Smaller (SALI) and the Generalized (GALI) Alignment Indices: Efficient Methods of Chaos Detection*. Berlin, Heidelberg: Springer Berlin Heidelberg, 2016. doi:10.1007/978-3-662-48410-4\_5
- [31] G. Russo, G. Franchetti, and M. Giovannozzi, “New Techniques to Compute the Linear Tune”, in *Proc. IPAC’21*, Campinas, SP, Brazil, 2021, pp. 4142–4145.  
doi:10.18429/JACoW-IPAC2021-THPAB189
- [32] G. Iadarola, Xsuite documentation pages, 2022. <https://xsuite.readthedocs.io>